Journal of Alloys and Compounds 489 (2010) 4–8

Contents lists available at ScienceDirect

Journal of Alloys and Compounds

journal homepage: www.elsevier.com/locate/jallcom

Thermoluminescence investigations in X-ray irradiated CaS phosphor

S. Adhikary, A. Choubey[*], S. Das, S.K. Sharma, J. Manam

Department of Applied Physics, Indian School of Mines University, Dhanbad 826004, India

ARTICLE INFO

Article history:
Received 2 June 2009
Received in revised form 1 September 2009
Accepted 2 September 2009
Available online 19 September 2009

PACS:
78.60.Kn
87.53.Dn

Keywords:
Phosphors
Solid-state reaction
Radiation effects
Luminescence
X-ray diffraction

ABSTRACT

We report the thermoluminescence studies of X-ray irradiated CaS phosphor. The CaS phosphor was prepared by solid-state diffusion method and characterized by X-ray diffraction technique (XRD), Fourier transform infrared spectroscopy (FTIR) and scanning electron microscopy (SEM). Thermally stimulated luminescence (TSL) glow curves of X-ray irradiated CaS sample have two glow peaks at temperatures 100 and 130 °C. A reliable dosimetric study of a thermoluminescence material is based on good knowledge of its trapping parameters. The trapping parameters namely activation energy, order of kinetics and frequency factor associated with the prominent glow peak (130 °C) of CaS phosphor were calculated by using isothermal decay and glow curve shape (Chen's) methods.

1. Introduction

The sulphide phosphors such as ZnS, SrS, and CaS have interesting properties useful for practical application, i.e. television screens, fluorescence lamps, thermoluminescence dosimetry, X-ray imaging screens, and high pressure mercury lamps [1–5]. Calcium sulphide is known as an afterglow phosphor with high luminescence efficiency and multiple luminescence centers. The CaS exhibits luminescence under irradiation at various wavelengths of light, X-rays, ultraviolet and visible light. The CaS phosphor has a large amount of defects such as S-vacancies and Ca-vacancies [6–8]. These defects are responsible for the thermoluminescence phenomenon in this phosphor. Keeping in view the application potentiality of CaS phosphor in different diverse fields, structural and thermally stimulated luminescence studies of this phosphor were carried out, which were not widely studied as evident from our literature survey. Moreover, the trapping parameters for this sample using the isothermal decay method are reported for the first time and the results are in good agreement with those obtained by Chen's glow curve shape method.

2. Experimental details

2.1. Sample preparation

The solid-state diffusion method was used to prepare CaS sample [9,10]. The sample was prepared by the reduction of alkaline earth sulphate to its sulphide by a reducing agent. Calcium sulphate was used as host system while carbon powder was used as reducing agent. The calcium sulphate powder was treated with nitric acid of analytical reagent (AR) grade. The powder was soaked in excess of dilute nitric acid (30%) and kept overnight. It was then heated for about half an hour to ensure the conversion of all metallic impurities into their respective nitrates. These soluble nitrates were eliminated by repeated washing in warm distilled water. The final powder was dried in an oven at about 60 °C and collected in bottles. After that the prepared powder and the reducing agent (carbon) were taken according to the proportion. These were mixed with the help of pestle and mortar. The mixture was packed in a quartz crucible and a thin layer of carbon powder spread over it. This was kept at 1000 °C temperature for 2 h. Finally, the prepared sample was cooled to room temperature by natural cooling and then the phosphor powder was collected in clean and dry sample tube.

2.2. Instruments

The characterization of the prepared sample was carried out by X-ray diffraction technique (XRD), scanning electron microscopy (SEM) and Fourier transform infrared spectroscopy (FTIR). X-ray diffractogram of this compound was taken at the room temperature in a wide range of Bragg angle 2θ ($10^\circ \leq 2\theta \leq 90^\circ$) using Rigaku X-ray diffractometer (Miniflex, Japan) at a scanning rate of 3°/min. The SEM study was carried out using FEI, QUANTA-300 electron microscope. The FTIR spectrum was recorded in the range 4000–400 cm^{-1} on FTIR-2000, Perkin Elmer Spectrophotometer. The thermally stimulated luminescence (TSL) studies were made by using thermoluminescence analyzer system supplied by Nucleonix Systems Private Limited, Hyderabad, India.

---

[*] Corresponding author. Tel.: +91 3262235412; fax: +91 3262296563.
E-mail address: anjani_physics@yahoo.com (A. Choubey).

0925-8388/$ – see front matter © 2009 Elsevier B.V. All rights reserved.
doi:10.1016/j.jallcom.2009.09.039

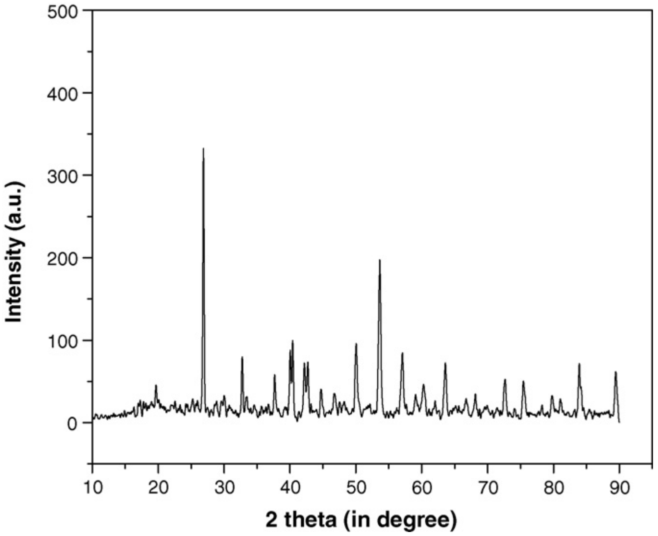

Fig. 1. XRD spectrum of CaS compound at room temperature.

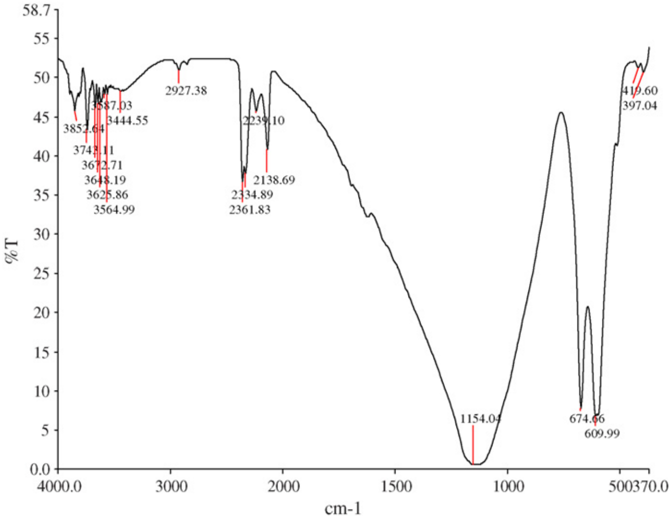

Fig. 3. FTIR spectrum of CaS compound at room temperature.

3. Results and discussion

3.1. XRD, SEM, FTIR, and TSL studies

The X-ray diffractogram of CaS compound is shown in Fig. 1. The sharp and single diffraction peaks of the XRD spectrum confirm the formation of single phase CaS compound. The CaS compound exhibited the cubic structure (space group $Pm\bar{3}m$) in correspondence with the JCPDS database of card number 01-078-1922 [11]. The diffraction peaks were indexed and unit cell configuration was identified using 'Powdmult'. The ($h\,k\,l$) values of most prominent diffraction peaks for CaS compound are (1 1 1), (3 1 0), (3 1 1), (2 2 2), (4 2 2) and (5 1 1). The lattice parameters of the unit cell for CaS compound were: $a = 5.69$ Å, $b = 5.69$ Å, $c = 5.69$ Å with $\alpha = 90^\circ$, $\beta = 90^\circ$, and $\gamma = 90^\circ$.

The SEM image of the prepared CaS compound is shown in Fig. 2. The image shows granular structure with particle sizes in the range of 2–5 μm. This non-uniform particle size is caused by the non-uniform distribution of temperature and mass flow during the synthesis. Moreover the particles have some angular edges. The powder sample can easily be termed as ultrafine because the size of these particles is less than 10 μm [12].

The FTIR spectrum of CaS compound is shown in Fig. 3. In a typical experiment 2–3 mg of the compound was mixed with about 80 mg of the KBr and then finally ground to a powder. The KBr pellets were obtained using a hydraulic pressure of 7–10 psi. The FTIR bands at 2361.83, 2334.89, 2239.10 and 2138.69 cm^{-1} are identified as S–H stretching bands [13]. According to Mikhlin et al. [14] the bands at 419 and 397 cm^{-1} can be assigned to elemental sulphur, polysulphide and disulphide species. Moreover, the peaks corresponding to $SO_4{}^{-2}$ bonding are observed at 1154.04, 674 and 610 cm^{-1} [13]. Characteristic bands around 3500 and 1630 cm^{-1} are due to atmospheric water vapor since KBr readily absorbs moisture from the air. Fortunately, these undesirable peaks (3500 and 1630 cm^{-1}) do not affect the identification of substance involved in this experiment due to different absorption positions of water and the possible product.

The TSL glow curves were recorded by X-ray irradiating the CaS phosphor for 15, 30, 45 and 60 s at room temperature (Fig. 4). The compound was heated at a uniform rate of 4 K/s with the help

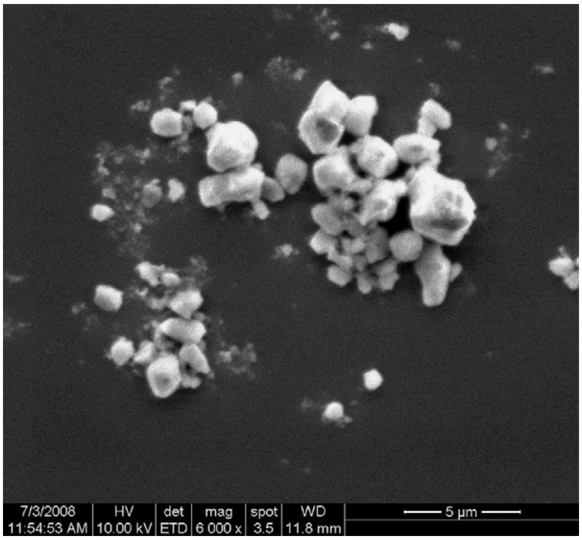

Fig. 2. SEM image of CaS compound at room temperature.

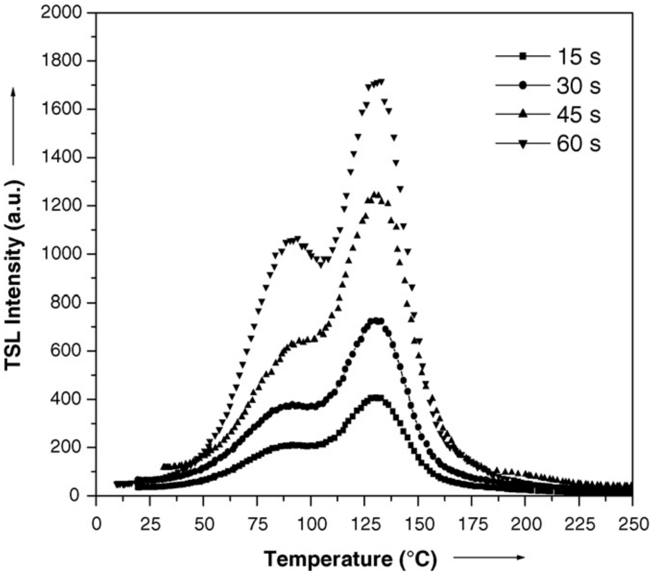

Fig. 4. TSL glow curves of CaS phosphor for different times of X-ray irradiation.

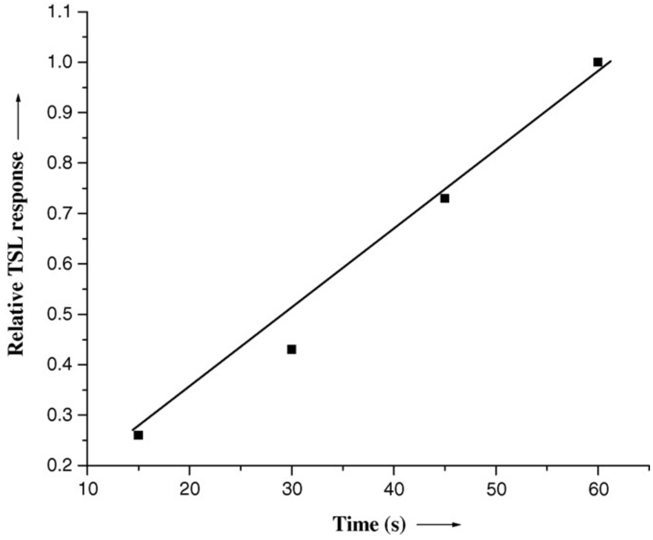

Fig. 5. Relative TSL response for 130 °C glow peak of CaS phosphor.

of a temperature controller and the luminescence emission was detected by a photo-multiplier (PM) tube. The photo-current from PM tube was amplified by a D.C. amplifier which was interfaced to a personal computer to obtain intensity vs temperature data. The radiation dose rate in our experimental studies was 50 mGy/min. The TSL glow curves exhibit simple structure with two glow peaks at temperatures 100 and 130 °C. The intensity and sharpness of 130 °C glow peak is greater than that of 100 °C glow peak. Moreover the intensities of the glow peaks are found to increase with increase of the X-ray irradiation dose.

The presence of two glow peaks in the TSL glow curves indicates that two different species of traps were being activated within the particular temperature range each with its own value of activation energy (E) and frequency factor (s). The peak temperature remains constant with increases of irradiation dose suggests that the glow peak follows first order kinetics as in the first order kinetics peak temperature (T_m) is independent of the initial number of trapped electrons (n_0), i.e. irradiation dose [15]. While in second order kinetics peak temperature (T_m) shifts towards lower temperature as irradiation dose increases. Again from Fig. 4 it is seen that the glow curve rises steadily to the peak and then falls rapidly to zero as the temperature rises, indicating that the curves are not symmetrical which again confirms that the glow peak at 130 °C is due to first order kinetics. In the first order process, the recombination probability of detrapped charge carrier with their counterpart has a constant value with time and hence the glow curves would not be symmetrical. Whereas in case of second order process, the light emission is delayed due to retrapping of charge carriers and it might be expected that the second order glow curve will display more luminescence during the second half of the peak than the first order curve, i.e. the second order glow curve would be nearly symmetrical.

The relative TSL intensity of 130 °C glow peak was plotted as a function of irradiation time and is shown in Fig. 5. The TSL dose dependence curve was observed to be almost linear in the studied range of irradiation time. The increase in the intensities of the glow peaks with increase of irradiation dose can be understood by the fact that more and more traps responsible for these glow peaks were getting filled with the increase of irradiation dose and subsequently these traps release the charge carriers on thermal stimulation to finally recombine with their counterparts, thus giving rise to different glow peaks.

3.2. *Trapping parameters*

Analysis of TSL glow curves has become important in view of the applications of thermoluminescence phenomena in dating, dosimetry and defect studies [16–19]. The determination of trapping parameters from the TSL glow curves is an active area of interest and various techniques have been developed for this. The trapping parameters namely activation energy (E), order of kinetics (b) and frequency factor (s) were calculated by using isothermal luminescence decay method [20]. As a check, the trapping parameters were also calculated by glow curve shape (Chen's) method.

3.2.1. *Isothermal luminescence decay method*

The isothermal luminescence decay method is based on recording the decay of luminescence intensity with respect to time at a constant temperature. Three temperatures were chosen on the rising side of the glow peak for which trapping parameters were to be determined. After irradiating the sample by an ionizing radiation with suitable dose, the sample was heated to one of the chosen temperature and decay of luminescence intensity was recorded at that temperature. The same procedure was repeated for other two chosen temperatures. The trapping parameters were evaluated by processing the experimental data.

3.2.1.1. First order kinetics. The TSL intensity equation for the first order kinetics is:

$$I = -\left(\frac{dn}{dt}\right) = ns\ \exp\left(-\frac{E}{kT}\right)$$

In this equation n is the concentration of trapped electrons at instant t, s is the frequency factor and E is the activation energy of trapped electrons.

The solution of intensity equation for the isothermal case:

$$I(t) = n_0 s\ \exp\left(-\frac{E}{kT}\right) \exp\left[-st\ \exp\left(-\frac{E}{kT}\right)\right]$$

Here n_0 is the concentration of trapped electrons at $t = 0$.

Or

$$\mathrm{Ln}\,[I(t)] = -\left[s\ \exp\left(-\frac{E}{kT}\right)\right] t + \left[\mathrm{Ln}\,(n_0 s) - \frac{E}{kT}\right] \qquad (1)$$

For the first order case, plot of Ln[$I(t)$] vs time should yield a straight line.

The slope of this straight line is:

$$m = s\ \exp\left(-\frac{E}{kT}\right)$$

or

$$\mathrm{Ln}[m(T)] = -\frac{E}{kT} + \mathrm{Ln}\,(s) \qquad (2)$$

The slope (m) of straight line plots of Ln[$I(t)$] vs time at different temperatures were noted and again Ln[$m(T)$] vs $1/T$ were plotted which was a straight line (Eq. (2)). The slope $m' = -E/k$ of this straight line give thermal activation energy (E) where k is the Boltzman's constant and intercept part Ln(s) of Eq. (2) gives the value of frequency factor (s).

3.2.1.2. General order kinetics. The TSL intensity equation for the general order kinetics is:

$$I = -\left(\frac{dn}{dt}\right) = s'n^b\ \exp\left(-\frac{E}{kT}\right)$$

where $s' = s/n_0^{b-1}$ is the pre-exponential factor and b is the order of kinetics.

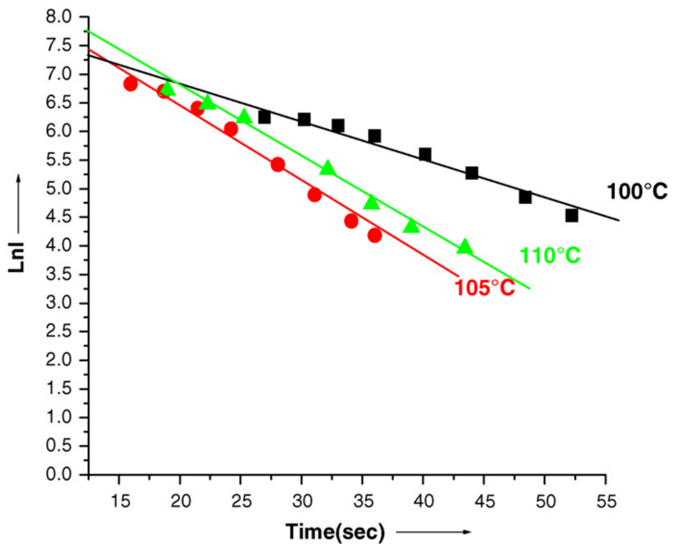

Fig. 6. Isothermal luminescence decay curves for 130 °C glow peak of CaS phosphor.

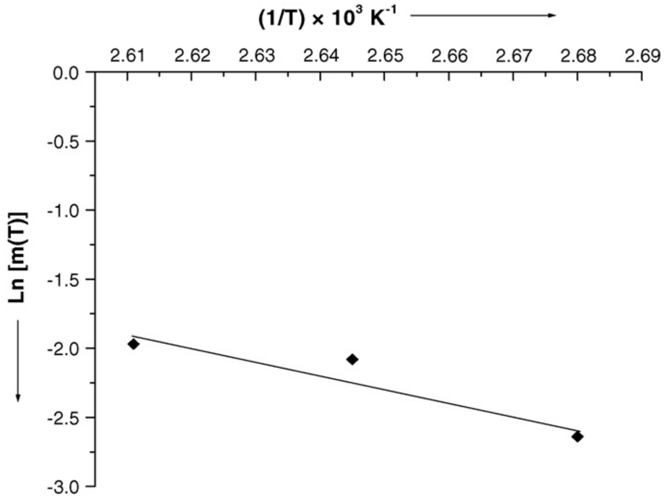

Fig. 7. Plot of Ln[$m(T)$] vs $1/T$ for 130 °C glow peak of CaS phosphor.

The solution of intensity equation for the isothermal case:

$$\left(\frac{I_0}{I}\right)^{b-1/b} - 1 = s\ \exp\left[-\frac{E}{kT}\right](b-1)t \tag{3}$$

so for the general order case, plot of $(I_0/I)^{(b-1)/b} - 1$ vs time should yield a straight line where b is the order of kinetics $(1 < b \leq 2)$, I_0 is the intensity at $t = 0$ and I is the intensity at any instant t. The experimental data was tested by choosing different test values of b, among which the value of b that gives the best fit as straight line gives the order of kinetics (b).

The slope of this straight line Eq. (3) is:

$$m = (b-1)s\ \exp\left(-\frac{E}{kT}\right) \tag{4}$$

The determination of slope (m) of straight line plots of $(I_0/I)^{(b-1)/b} - 1$ vs time at different temperatures will give the value of frequency factor according to the relation:

$$s = \frac{(m_2)^{T_2/(T_2-T_1)}}{(b-1)(m_1)^{T_1/(T_2-T_1)}} \tag{5}$$

where m_1 and m_2 are the slopes corresponding to the temperatures T_1 and T_2 respectively.

From Eq. (4):

$$\mathrm{Ln}[m(T)] = -\frac{E}{kT} + \mathrm{Ln}[s(b-1)] \tag{6}$$

Now to find the thermal activation energy (E) a graph Ln[$m(T)$] vs $1/T$ was plotted, which was a straight line (Eq. (6)). The slope $m' = -E/k$ of this straight line graph gives the value of thermal activation energy (E).

In order to calculate the trapping parameters corresponding to the 130 °C glow peak (Fig. 4) by isothermal luminescence decay method, three temperatures namely 100, 105 and 110 °C were chosen on the rising side of the glow peak and the decay of luminescence intensity with time at these temperatures were recorded, the sample previously having been irradiated for 1 min under the conditions of 20 kV and 15 mA. The plots of Ln I vs time at these temperatures provide best straight line fits (Fig. 6), thereby establishing that the glow peak at 130 °C obey first order kinetics. To confirm the above result, plots of $(I_0/\mathrm{I})^{(b-1)/b} - 1$ vs time were drawn for different values of b $(1 < b \leq 2)$. It was found that these plots did not exhibit straight line nature, which indicates that this peak does not obey general or second order kinetics. The best straight line fitting was obtained for the Ln I vs time plots, which established that 130 °C glow peak obeys first order kinetics.

In order to find the thermal activation energy (E) and frequency factor (s), slopes (m) of straight line plots of Ln I vs time (Fig. 6) were obtained for the three temperatures namely 100, 105 and 110 °C. These slopes were plotted as Ln(m) vs $1/T$ which yields a straight line (Fig. 7). The activation energy (E) as well as frequency factor (s) were calculated from the slope ($m' = -E/k$) and intercept part Ln(s) of this straight line and were found to be 0.83 eV and 1.65×10^{10} s^{-1} respectively.

3.2.2. *Glow curve shape method*

In order to calculate the trapping parameters associated with the 130 °C glow peak by glow curve shape method, the peak is to be isolated from the 100 °C peak. This was done using the thermal cleaning technique [21]. For this, the sample was X-irradiated for 60 s at room temperature and then heated up to 100 °C and after that TSL glow curve was recorded which exhibits one isolated peak at 130 °C. This isolated peak was normalized to the required height of the composite glow curve for 60 s.

3.2.2.1. Order of kinetics. Order of kinetics (b) was determined by calculating the symmetry factor (μ_g) and Balarin parameter (γ) of the glow peak from the known values of shape parameters:

$$\mu_g = \frac{\delta}{\omega} = \frac{T_2 - T_m}{T_2 - T_1} \tag{7}$$

$$\gamma = \frac{\delta}{\tau} = \frac{T_2 - T_m}{T_m - T_1} \tag{8}$$

Table 1 gives the values of shape parameters (τ, δ, ω) of the 130 °C glow peak of CaS phosphor.

The shape factor (μ_g) for the 130 °C glow peak of CaS phosphor was calculated using above equation and was found to be ∼0.42. This value suggests that this peak obey first order kinetics ($b = 1$), which implies that the process of retrapping is negligible and the traps are situated very close to the luminescence centre.

Furthermore, Balarin parameter (γ) ranges from 0.7 to 0.8 for a first order kinetics and from 1.05 to 1.20 for a second order kinetics

Table 1
Shape parameters of 130 °C glow peak of CaS phosphor.

τ (K)	δ (K)	ω (K)
$T_m - T_1 = 24.7$	$T_2 - T_m = 18.34$	$T_2 - T_1 = 43.04$

[22]. This parameter (γ) for the 130 °C glow peak of CaS was found to be 0.74 which further suggest that this peak obey first order kinetics.

3.2.2.2. Activation energy. Activation energy (E) was calculated by using the Chen's equations [23] for first order glow peaks which gives the trap depth in terms of τ, δ, ω. A general formula for E was given by:

$$E = \frac{c_\gamma k T_m^2}{\gamma} - b_\gamma 2kT_m \tag{9}$$

where γ is τ, δ or ω. The constants c_γ and b_γ for the three equations (τ, δ and ω) and for first order kinetics are $C_\tau = 1.51$, $b_\tau = 1.58$, $C_\delta = 1.51$, $b_\delta = 0$, $C_\omega = 2.52$, and $b_\omega = 1.0$.

The activation energy for the 130 °C glow peak of CaS phosphor, when calculated using Eq. (9) by considering low temperature half width, high temperature half width and full width of the peak at its half height, was found to be 0.84 eV in average.

3.2.2.3. Frequency factor. Once the order of kinetics and activation energy were determined, the frequency factor (s), which expresses the product of frequency with which the electrons strike the sides of the potential well of the trap and the reflection coefficient, was calculated using the equation given by Chen and Winer [24]:

$$\frac{qE}{kT_m^2} = s\left[1 + (b-1)\frac{2kT_m}{E}\right]\exp\left(-\frac{E}{kT_m}\right) \tag{10}$$

where q is the heating rate.

The frequency factor for the 130 °C glow peak of CaS phosphor was found using Eq. (10) to be $0.8 \times 10^{10}\ \mathrm{s}^{-1}$.

4. Conclusions

In dosimetry, the phosphors are required which exhibit simple and sharp glow curves, linear TL dose–response and whose sensitivity is large even in the low radiation range. From the present studies, CaS has been found to have simple and sharp glow peaks, good linearity in TL dose–response, excellent TL sensitivity under low radiation doses and moreover, it can be prepared very easily and thus can be used in the radiation dosimetry. The results of the trapping parameters calculated by the two different methods are in good agreement indicating the reliability of the methods used.

References

[1] H.-J. Sung, Y.-S. Cho, Y.-D. Huh, Y.R. Do, Bulletin of Korean Chemical Society 28 (8) (2007) 1280.
[2] H.S. Bhatti, R. Sharma, N.K. Verma, Journal of Modern Optics 53 (14) (2006) 2021.
[3] H.S. Bhatti, R. Sharma, N.K. Verma, Radiation Effects and Defects in Solids 161 (2) (2006) 113.
[4] A.G.J. Green, B. Ray, I.V.F. Viney, J.W. Brightwell, Physica Status Solidi (a) 110 (1) (2006) 269.
[5] X. Zhaoxian, C. Yayong, C. Zhihui, S. Chunxiao, Journal of Rare Earths 24 (1) (2006) 133.
[6] N. Singh, G.L. Marwaha, V.K. Mathur, Physica Status Solidi (a) 66 (2) (2006) 761.
[7] Y. Kojima, K. Aoyagi, T. Yasue, Journal of Luminescence 126 (2) (2007) 319.
[8] C. Guo, D. Huang, Q. Su, Material Science and Engineering B 130 (1–3) (2006) 189.
[9] V. Singh, T.K. GunduRao, J.-J. Zhu, M. Tiwari, Material Science and Engineering B 131 (1–3) (2006) 195.
[10] V. Kumar, R. Kumar, S.P. Lochab, N. Singh, Radiation Effects and Defects in Solids 161 (8) (2006) 479.
[11] H. Luo, R.G. Greene, Ghandehari, Physics Review B: Solid State 5 (1994) 16233.
[12] D. Jia, Ph.D. Thesis, Material Science, Department of Geo. and Phys., Lock Haven Univ. of Pennsylvania.
[13] B. Smith, Infrared Spectral Interpretation: A Systematic Approach, CRC Press, New York, 1999.
[14] Yu.L. Mikhlin, A.V. Kuklinskiy, N.I. Pavlenko, Geochimica et Cosmochimica Acta 66 (2003) 4057.
[15] R. Chen, S.W.S. McKeever, Theory of Thermoluminescence and Related Phenomena, World Scientific, Singapore, 1997.
[16] Y.S. Horowitz, Thermoluminescence and Thermoluminescent Dosimetry, Franklin Book Company, Incorporated, 1984.
[17] J.R. Cameron, G.N. Kenney, Radiation Research 19 (1963) 199.
[18] M.J. Aitkens, Thermoluminescence Dating, Academic Press, 1985.
[19] R. Chen, Y. Kirsh, Analysis of Thermally Stimulated Processes, Pergamon, Oxford, 1981.
[20] S.K. Sharma, Ph.D. Thesis, I.S.M. University, Dhanbad, 2005.
[21] S.W.S. Mckeever, Thermoluminescence in Solids, Cambridge University Press, 1985.
[22] M. Balarin, Journal of Thermochemical Analysis 17 (1979) 319.
[23] R. Chen, Journal of Applied Physics 40 (1969) 570.
[24] R. Chen, S.A.A. Winer, Journal of Applied Physics 41 (1970) 5227.